

Scaling Theory of Two-Phase Dendritic Growth in Undercooled Ternary Melts

Silvère Akamatsu,^{1,2,*} Sabine Bottin-Rousseau,¹ Gabriel Faivre,^{1,2} and Efim A. Brener³

¹*Institut des Nanosciences de Paris, UMR 7588, Sorbonne Universités/UPMC, 4 place Jussieu, 75005 Paris, France*

²*INSP, UMR 7588, CNRS, 4 place Jussieu, 75005 Paris, France*

³*Peter Grünberg Institut, Forschungszentrum Jülich, D-52425 Jülich, Germany*

(Received 6 November 2013; published 11 March 2014)

Two-phase dendrites are needlelike crystals with a eutectic internal structure growing during solidification of ternary alloys. We present a scaling theory of these objects based on Ivantsov's theory of dendritic growth and the Jackson-Hunt theory of eutectic growth. The additional introduction of the relationship $\rho \sim \lambda$ (ρ : dendrite tip radius; λ : eutectic interphase spacing) suggested by recent experimental results [S. Akamatsu *et al.*, Phys. Rev. Lett. **104**, 056101 (2010)] leads to a complete solution of the selection problem and to the scaling rule $\rho \sim v^{-1/2}$ (v : dendrite tip growth rate).

DOI: 10.1103/PhysRevLett.112.105502

PACS numbers: 81.10.Aj, 68.70.+w, 81.30.Fb

The term “two-phase dendrite” is used in materials sciences to designate needle-shaped crystals with a fine two-phase internal structure like those observed during univariant solidification of three-component alloys [1,2]. Few detailed studies have so far been devoted to these objects. The first theoretical questions that have to be dealt with are whether two-phase dendrites can grow in a stationary way and, if so, whether anisotropy effects are crucial in the process. An answer to these questions has recently been provided by the finding of stationary *spiral* two-phase dendrites (*sp* dendrite) during directional solidification of a transparent nonfaceted ternary eutectic [3,4]. The properties of the *sp* dendrites are illustrated in Fig. 1. Like one-phase dendrites, they can be subdivided into a tip region characterized by a smooth outer shape, and a tail region where this shape is disrupted by morphological instabilities. In the tip region, the outer shape is a paraboloid. The two-phase substructure is generated by a spiral eutectic pattern located at the tip and rotating at a constant rotation speed. Except close to the tip, an interphase spacing λ , which is approximately equal to the helix pitch, can be defined. More details are given below. For now, we simply stress the fact that the spiral mechanism makes possible a perfectly steady two-phase growth along the curved solid-liquid interface, and that this mechanism in no way involves anisotropy effects. This has recently been confirmed by phase-field numerical simulations of *sp* dendrites performed in a model ternary system in which the level of interfacial anisotropy could be varied [5].

In this Letter we present a scaling theory of the steady state of two-phase dendrites in free growth in a ternary system without surface tension anisotropy. Our main objective is to cast light on the mechanism of selection and the range of existence of this growth structure in terms of morphological and thermodynamical parameters. The paraboloid outer shape and the regular eutectic substructure of *sp* dendrites suggest viewing the diffusion field outside

two-phase dendrites as being composed of two parts: a long-range field, which only depends on the average composition of the liquid along the envelope of the dendrite, and obeys a theory similar to that of one-phase dendrites; a short-range field, which is driven by the differences in concentration in the liquid in front of the two eutectic phases, and is relevant to a theory similar to that of lamellar eutectic growth. We begin with a brief summary of these theories.

Consider the free growth of a one-phase dendrite in an AX binary alloy, where X is the solute. As a first step, the theory assumes that surface-tension effects are negligible.

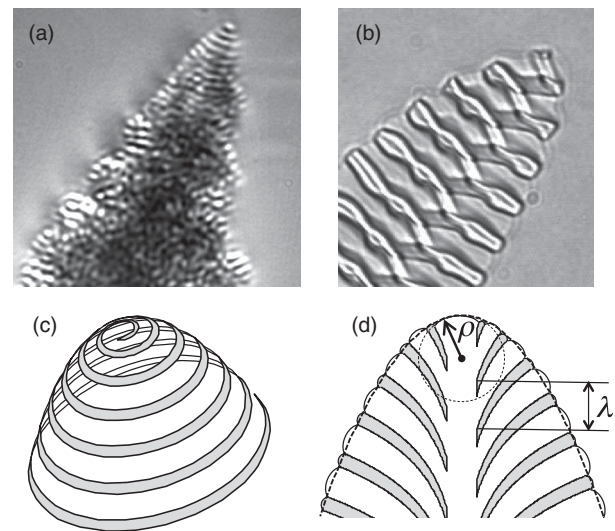


FIG. 1. Spiral two-phase dendrites. (a) and (b) *In situ* optical micrographs taken during directional solidification of a transparent ternary alloy (for experimental details, see [3]). (a) Bulk sample, horizontal dimension 105 μm . (b) Thin sample, horizontal dimension, 65 μm . (c) Schematic 3D representation of the solid-liquid interface. One of the solid phases is gray, the other white. (d) Longitudinal section of the internal microstructure (dotted line shows the parabolic envelope).

This implies that the solid-liquid interface is an isoconcentration surface, and that the solute mole fractions (for short, concentrations) of the liquid and the solid are those of the liquidus and solidus at the temperature T of the system. Let x and x_s be these concentrations, respectively, and x_∞ be the solute concentration far from the dendrite. Let v be the growth speed of the dendrite tip, ρ the tip radius, D_x the diffusion coefficient of X in the liquid, and

$$\Delta_x = \frac{x - x_\infty}{x - x_s} \quad (1)$$

the degree of supersaturation of the liquid. Ivantsov demonstrated that all the paraboloids such that

$$\frac{v\rho}{D_x} = F^{lv}(\Delta_x), \quad (2)$$

where $F^{lv}(\Delta_x) \sim \Delta_x / \ln(\Delta_x^{-1})$, when $\Delta_x \ll 1$ (which is the case we consider here), are steady-state solutions of the equations of growth without surface-tension effects [6]. In the next step an additional equation of the form $\rho^2 v = \text{const}$ is provided by introducing slightly anisotropic surface-tension or kinetic effects. As a result, v and ρ are uniquely determined and linked by a $\rho \sim v^{-1/2}$ scaling relationship at given Δ_x . This has been established for both 2D [7–10] and 3D dendrite growth [11,12]. Similar selection and scaling rules for v and ρ have been found for various other needlelike crystal growth shape, such as the doublon (also called double finger) [13,14] and the two-phase finger [15,16]. Unlike the dendrite, these last growth shapes are not crucially dependent on interfacial anisotropy and are not selected in orientation. On the other hand, like the dendrite, their shape does not depart much from an Ivantsov paraboloid, except at the tip, where a specific local structure ensures their stabilization and speed selection.

Consider now an AB binary alloy, where B is the solute, having a eutectic plateau at some temperature T_E and a global concentration c_∞ falling well inside this plateau. The growing solid contains two different crystal phases, namely, an A -rich α phase and a B -rich β phase. At small solidification rates the system admits steady states consisting of a planar $\alpha\beta$ growth front with a uniform spacing λ and a small average undercooling with respect to T_E . We summarize the Zener-Hillert-Jackson-Hunt (JH) theory of these states [17]. This theory was formulated for directional solidification in the $G/V \rightarrow 0$ limit and thus also holds in free growth. It is valid under the condition that $\lambda V/D \ll 1$, where D is the diffusion coefficient of B in the liquid, which was verified during the experimental observation of sp dendrites. The average concentration c^α of the liquid in front of the α -liquid interfaces is larger than the average concentration c^β in front of the β -liquid ones at the temperature T of the growth front. This forms the basis of the exchange of solute between solid phases during growth. To a good approximation, c^α is on the α liquidus of

the alloy and therefore is in equilibrium with a point c_s^α of the α solidus. The same applies to c^β mutatis mutandis. JH showed that the mass conservation equation at the interface leads to

$$P \frac{\lambda V}{D} = \Delta^{\text{sol}}, \quad (3)$$

where

$$\Delta^{\text{sol}} = \frac{c^\alpha - c^\beta}{c_s^\beta - c_s^\alpha} \quad (4)$$

and P is a small (< 0.1) numerical factor occurring from the summation over the periodic structure. Note, incidentally, that the fraction η of β phase in the solid is related to c_∞ by the global mass conservation equation $c_\infty = \eta c_s^\beta + (1 - \eta) c_s^\alpha$. Furthermore, capillary effects (namely, the interface equilibrium conditions at the α - β -liquid junctions) generate a mean curvature of the solid-liquid interface. This gives an additional “capillary” contribution to the average undercooling of the growth front, which reads

$$\frac{d_0}{\lambda} = \Delta^{\text{cap}}, \quad (5)$$

where d_0 is a material-dependent capillary length. The spacing value $\lambda_{\text{JH}} = \sqrt{P^{-1} d_0 D V^{-1}}$ at which

$$\Delta^{\text{sol}} = \Delta^{\text{cap}} = \frac{\Delta_E}{2} \quad (6)$$

is an important characteristic length for eutectic growth patterns. To be sure, there is no “strong selection” (in the sense that λ tends towards λ_{JH} , or a value close to λ_{JH} , over time at constant V) of the spacing in binary eutectic growth, contrary to what was long believed. However, it is also true that any local structure containing λ values deviating from λ_{JH} by a factor of more than about 2 is short lived, so that, broadly speaking, λ is almost always close to λ_{JH} , a fact which is sometimes referred to as “weak selection” [18–20].

Consider finally the directional solidification of an $\alpha\beta$ solid in an ABX ternary alloy, as studied in Ref. [3]. The rejection of X into the liquid during growth generated a concentration gradient that caused a large-scale (compared to λ) Mullins-Sekerka-like instability of the $\alpha\beta$ growth front at values of V larger than a threshold value V_c [21,22]. Spiral two-phase dendrites were observed at $V \gg V_c$ and appeared in the form of isolated objects. Their tip region was thus growing under nearly free-growth (virtually zero G/V and infinite primary spacing) conditions [23–25]. The theory presented herein should, therefore, be applicable to them. Their growth direction, like those of doublons and two-phase fingers, was not fixed, but history dependent,

meaning that different sp dendrites had different values of their tip growth rate v at fixed V . The explored v range was $0.1\text{--}1\ \mu\text{m s}^{-1}$. The tip radius ρ of the sp dendrites was measured by fitting a parabola to the contour of the images. The extension of the tip region was between 5 and $10\ \rho$. The spacing λ was determined as the product of v and the period of rotation of the spiral pattern. The measured λ values turned out to be within 10% of the λ_{JH} ones for the AB binary alloy ($\lambda_{\text{JH}}^2 V \approx 10.2\ \mu\text{m}^3\text{ s}^{-1}$) over the whole experimental v range. The ρ values showed a similar variation, with $\rho \approx 0.75\lambda_{\text{JH}}$ on average. Most importantly, two sp dendrites growing simultaneously, side by side, had the same values of λ , ρ , and tip temperature. There is thus a clear indication of a strong selection of both the tip radius and the eutectic spacing of sp dendrites according to a $\lambda \sim \rho \sim v^{-1/2}$ law.

We now come to the theory of two-phase dendrite growth. c will designate a concentration of B , x a concentration of X , and a pair (c, x) a composition of the alloy. Concentrations in the solid phases will be tagged by a subscript s and average concentrations along the growth front by a bar. As a first step, we consider the long-range concentration field of a sp dendrite. For ease of exposition, we assume that there is no cross diffusion in the liquid and that the diffusion coefficients of B and X , called D and D_x , respectively, have the same order of magnitude, as is in fact often the case in the experiments. Then an Ivantsov equation holds for each component separately: we have

$$\frac{v\rho}{D} = F^{Iv}(\Delta_c), \quad \frac{v\rho}{D_x} = F^{Iv}(\Delta_x), \quad (7)$$

where

$$\Delta_c \sim \frac{\bar{c} - c_\infty}{\bar{c} - \bar{c}_s}, \quad \Delta_x \sim \frac{\bar{x} - x_\infty}{\bar{x} - \bar{x}_s}. \quad (8)$$

The average concentration \bar{x} is defined by the equation

$$\bar{x} = \eta x^\beta + (1 - \eta)x^\alpha, \quad (9)$$

where η is unknown. Similar equations hold for \bar{c} , \bar{c}_s , and \bar{x}_s . By the elimination of $v\rho$, Eqs. (7) lead to a relationship between Δ_c and Δ_x , and thus between the average concentrations. Knowing that $D_x \approx D$, we rewrite Eqs. (7) in the form

$$\Delta_c \sim \Delta_x, \quad (10)$$

and

$$\frac{v\rho}{D} \sim \frac{\Delta_x}{\ln(\Delta_x^{-1})}. \quad (11)$$

Regarding the short-range part of the concentration field, we approximate the spiral substructure near the dendrite tip by some effective lamellar structure. The resulting

uncertainty in the definition of λ and v is within the limits of the scaling theory proposed here. Then, according to Eqs. (3) and (5), and assuming that $\lambda/\lambda_{\text{JH}}$ is kept constant at a value close to 1 in agreement with the experimental measurements:

$$P \frac{\lambda v}{D} \sim \Delta_E, \quad (12)$$

and

$$\frac{d_0}{\lambda} \sim \Delta_E, \quad (13)$$

where Δ_E is given by Eqs. (4) and (6). There are apparently twelve unknown concentration variables in Eqs. (10) to (13), but their actual number is only two due to the four relationships defining the average concentrations and the six relationships giving, for each phase, three equilibrium concentrations as a function of the fourth one. Thus, at this stage there are six unknowns, say, x^α , x^β , η , v , ρ , and λ , at fixed (c_∞, x_∞) , and four relationships between them.

We now look for additional relationships. Figure 2 schematically represents the isothermal section of the ABX phase diagram at the temperature T . It features two two-phase domains delimited by the intersections of the liquidus and solidus surfaces by the T plane, the point of intersection (c_u, x_u) of the univariant groove with the T plane, the points $(c_{su}^\alpha, x_{su}^\alpha)$ and $(c_{su}^\beta, x_{su}^\beta)$ on the solidus lines that are in equilibrium with (c_u, x_u) , and the triangular three-phase domain delimited by the conjugation lines between, (c_u, x_u) , $(c_{su}^\alpha, x_{su}^\alpha)$, and $(c_{su}^\beta, x_{su}^\beta)$.

For the sake of clarity, we begin by considering the particular case of a system having $A \leftrightarrow B$ symmetry [Fig. 3(a)]. In other words, we assume that the isothermal section of the phase diagram is symmetrical with respect to the $x = 1 - 2c$ axis and that (c_∞, x_∞) is on this axis. Incidentally, these conditions were approximately fulfilled in the experimental system in which sp dendrites were

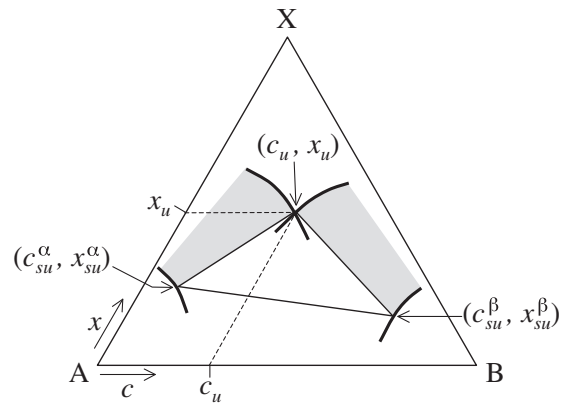


FIG. 2. Isothermal section of the phase diagram of the ABX alloy in Gibbs' triangular coordinates. Grey areas: two-phase domains. Triangle: three-phase domain.

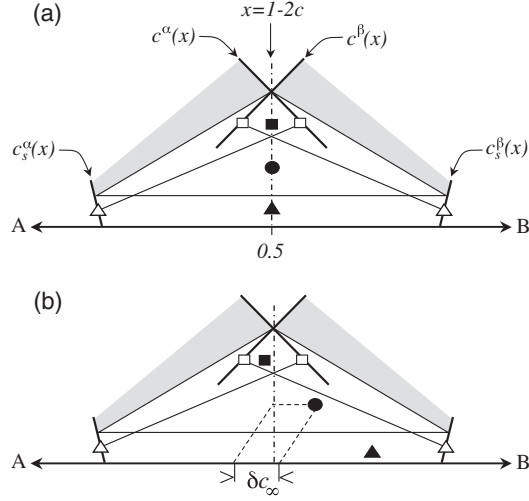


FIG. 3. Isothermal section of a phase diagram having $A \leftrightarrow B$ symmetry. (a) Symmetrical system. (b) Symmetry-broken system. Closed circles: (c_∞, x_∞) . Closed squares: (\bar{c}, \bar{x}) . Closed triangles: (\bar{c}_s, \bar{x}_s) . Open squares: (c^α, x^α) and (c^β, x^β) . Open triangles: (c_s^α, x_s^α) and (c_s^β, x_s^β) .

observed. Under these conditions, the sp dendrites must satisfy the symmetry requirements $\eta = 1/2$ and $x^\alpha = x^\beta$. The number of unknowns is now four, say, \bar{x} , v , ρ , λ . On the other hand, the $A \leftrightarrow B$ symmetry also imposes that $\bar{x} = 1 - 2\bar{c}$ and $\bar{x}_s = 1 - 2\bar{c}_s$, so that Eq. (10) becomes an identity and is no longer part of the equations of the problem. One additional relationship arising from the interaction between the long-range and the short-range dynamics must be found. The experiments clearly suggest that there is a linear, or almost linear, relationship between λ and ρ . We therefore write

$$\lambda \sim \rho. \quad (14)$$

Given that $\lambda \sim \lambda_{JH}$, Eq. (14) also implies that $\lambda \sim \rho \sim v^{-1/2}$. Presumably, Eq. (14) arises from the fact that sp dendrites cannot grow with $\rho \ll \lambda$ for geometrical reasons while, on the other hand, sp dendrites with $\rho \gg \lambda$ are unstable with respect to a decrease in ρ that would make them grow faster. So, the only ρ vs λ range in which sp dendrites can stabilize is the one given by Eq. (14).

From Eqs. (11), (12), and (14) one finally obtains

$$\Delta_E \sim \frac{P \Delta_x}{\ln(\Delta_x^{-1})}. \quad (15)$$

Both the quantities P and $1/\ln(\Delta_x^{-1})$ are substantially smaller than unity. Thus, $\Delta_E/\Delta_x \ll 1$ and $x_u - \bar{x} \ll 1$. We can therefore approximate Δ_x as

$$\Delta_x \approx \frac{x_u - x_\infty}{x_u - x_{su}}. \quad (16)$$

Plugging this relationship into (15), it can be seen that Δ_x and Δ_E , i.e., the driving forces for growth, now depend

only on control and material parameters. Expanding the equilibrium equations to the first order in $x - x_u$ near the univariant points, one obtains from Eq. (8)

$$x_u - \bar{x} \sim \frac{c_{su}^\beta - c_{su}^\alpha}{2|\partial c^\alpha / \partial x_u| - 1} \Delta_E, \quad (17)$$

which yields \bar{x} as a function of the control and material parameters. Then one gets from Eqs. (12), (13), and (14)

$$v \sim \frac{D}{P d_0} \Delta_E^2 \quad (18)$$

and

$$\lambda \sim \rho \sim \frac{d_0}{\Delta_E}, \quad (19)$$

which completely solves the selection problem. As a last remark, we put Eq. (17) into the form

$$x_u - \bar{x} \sim K(x_u - x_\infty). \quad (20)$$

It can be seen from Eqs. (15), (16), and (17) that K is the product of $P/\ln(\Delta_x^{-1})$ and some material parameters that generally are on the order of unity. Thus, in general, $K \ll 1$ and \bar{x} is much closer to x_u than x_∞ .

In the case of systems without any particular symmetry, there are two more independent unknowns (say, η and $x^\alpha - x^\beta$) and one more relationship than in symmetrical systems. One additional relationship is thus required for determining all the unknowns uniquely. However, this relationship is about the details of the short-range field and is of little consequence as regards the domain of existence of two-phase dendrites. As an exploratory suggestion, we therefore set $x^\alpha - x^\beta$ to zero. Keeping the same symmetrical phase diagram as above, we introduce a small departure δc_∞ of the alloy concentration from the axis of symmetry and calculate the departures of η , \bar{c} , and \bar{c}_s from their values at $\delta c_\infty = 0$. Expanding Eqs. (8) and (10) to first order and using the fact that $\Delta_E \ll \Delta_x$, one gets $\delta \bar{c} \sim -\delta c_\infty \Delta_E / \Delta_x$, $\delta \bar{c}_s \sim \delta c_\infty / \Delta_x$ and

$$\delta \eta \sim \frac{\delta c_\infty}{(c_{su}^\beta - c_{su}^\alpha) \Delta_x}. \quad (21)$$

It is interesting to note that $\delta \eta$, $\delta \bar{c}_s$, and δc_∞ have the same sign and that $|\delta \bar{c}_s|$ is substantially larger than $|\delta c_\infty|$. When, for instance, δc_∞ is positive, the dendrite is, on average, more enriched in B than the liquid. The concentration range of existence of sp dendrites, as determined by Eq. (21) and the condition $|\delta \eta| < 0.5$, is delimited by the conjugation lines $(c^\sigma, x^\sigma) - (c_s^\sigma, x_s^\sigma)$. Thus, as \bar{x} is close to x_u , the range of existence of sp dendrites roughly coincides with the three phase domain [Fig. 3(b)]. The operating point of the dendrite tip remains close to the univariant groove of the

phase diagram as the alloy composition goes through this domain.

In conclusion, we have obtained a complete solution of the selection problem for two-phase dendrites on the condition of postulating a relationship linking the tip radius of the dendrite to the interphase spacing of the eutectic microstructure. This relationship reads $\rho \sim \lambda$ and is based on the geometry of the source of the eutectic patterns located at the tip of the dendrite. This very natural length scale selection by the underlying eutectic structure replaces the much more delicate surface tension anisotropy mechanism that takes place in one-phase dendrites (the so-called microscopic solvability criterion). No particular condition appears to be required for the alloy to display two-phase dendrites beyond the fact that its composition is close to a univariant groove of the phase diagram and that it solidifies in a nonfaceted way. This suggests that *sp* dendrites should be a common occurrence in univariantly solidified ternary eutectics.

We thank M. Plapp, G. Boussinot, L. Gránásy, and T. Pusztai for fruitful discussions. E. A. B. benefited from an invited-professor position at UPMC. This work was supported by the Centre National d'Etudes Spatiales, France.

*akamatsu@insp.jussieu.fr

- [1] U. Hecht, L. Gránásy, T. Pusztai, B. Böttger, M. Apel, V. Witusiewicz, L. Ratke, J. De Wilde, L. Froyen, D. Camel, B. Drevet, G. Faivre, S. G. Fries, B. Legendre, and S. Rex, *Mater. Sci. Eng. R* **46**, 1 (2004).
- [2] M. D. Rinaldi, R. M. Sharp, and M. C. Flemings, *Metall. Trans.* **3**, 3139 (1972).
- [3] S. Akamatsu, M. Perrut, S. Bottin-Rousseau, and G. Faivre, *Phys. Rev. Lett.* **104**, 056101 (2010).
- [4] L. Sturz, V. T. Witusiewicz, U. Hecht, and S. Rex, *J. Cryst. Growth* **270**, 273 (2004).
- [5] T. Pusztai, L. Rátkai, A. Szállás, and L. Gránásy, *Phys. Rev. E* **87**, 032401 (2013).
- [6] G. P. Ivantsov, *Dokl. Akad. Nauk SSSR* **58**, 567 (1947).
- [7] M. Ben Amar and Y. Pomeau, *Europhys. Lett.* **6**, 609 (1988); See also, D. Kessler, J. Koplik, and H. Levine, *Adv. Phys.* **37**, 255 (1988).
- [8] E. A. Brener, *J. Cryst. Growth* **99**, 165 (1990).
- [9] E. A. Brener and V. I. Mel'nikov, *Adv. Phys.* **40**, 53 (1991).
- [10] Y. Pomeau and M. Ben Amar in *Solids Far from Equilibrium*, edited by C. Godrèche, (Cambridge University Press, Cambridge, England, 1992), p. 365.
- [11] M. Ben Amar and E. A. Brener, *Phys. Rev. Lett.* **71**, 589 (1993).
- [12] E. A. Brener, *Phys. Rev. Lett.* **71**, 3653 (1993).
- [13] M. Ben Amar and E. A. Brener, *Phys. Rev. Lett.* **75**, 561 (1995).
- [14] S. Akamatsu, G. Faivre, and T. Ihle, *Phys. Rev. E* **51**, 4751 (1995).
- [15] S. Akamatsu and G. Faivre, *Phys. Rev. E* **61**, 3757 (2000).
- [16] G. Boussinot, C. Hüter, and E. A. Brener, *Phys. Rev. E* **83**, 020601(R) (2011).
- [17] K. A. Jackson and J. D. Hunt, *Trans. Metall. Soc. AIME* **236**, 1129 (1966), and references therein.
- [18] A. Karma and A. Sarkissian, *Metall. Mater. Trans. A* **27A**, 635 (1996).
- [19] M. Ginibre, S. Akamatsu, and G. Faivre, *Phys. Rev. E* **56**, 780 (1997).
- [20] S. Akamatsu, M. Plapp, G. Faivre, and A. Karma, *Phys. Rev. E* **66**, 030501 (2002).
- [21] W. W. Mullins and R. F. Sekerka, *J. Appl. Phys.* **35**, 444 (1964).
- [22] M. Plapp and A. Karma, *Phys. Rev. E* **60**, 6865 (1999); *Phys. Rev. E* **66**, 061608 (2002).
- [23] Y. Saito, C. Misbah, and H. Müller-Krumbhaar, *Phys. Rev. Lett.* **63**, 2377 (1989).
- [24] S. Akamatsu and T. Ihle, *Phys. Rev. E* **56**, 4479 (1997).
- [25] S. Gurevich, A. Karma, M. Plapp, and R. Trivedi, *Phys. Rev. E* **81**, 011603 (2010).